MOLECULAR IMAGING AND BIOLOGY

World Molecular Imaging Society
esmi — imaging life — European Society for Molecular Imaging
CrossMark

RESEARCH ARTICLE

Clinical Translation of [68Ga]Ga-NOTA-anti-MMR-sdAb for PET/CT Imaging of Protumorigenic Macrophages

Catarina Xavier,[1] Anneleen Blykers,[1] Damya Laoui,[2,3] Evangelia Bolli,[2,3] Ilse Vaneyken,[1,4] Jessica Bridoux,[1] Henri Baudhuin,[1] Geert Raes,[2,3] Hendrik Everaert,[4] Kiavash Movahedi,[2,3] Jo A. Van Ginderachter,[2,3] Nick Devoogdt,[1] Vicky Caveliers,[1,4] Tony Lahoutte,[1,4] Marleen Keyaerts [1,4]

[1]*In Vivo Cellular and Molecular Imaging Laboratory (ICMI), Vrije Universiteit Brussel, Brussels, Belgium*
[2]*Lab of Cellular and Molecular Immunology, Vrije Universiteit Brussel, Brussels, Belgium*
[3]*Myeloid Cell Immunology Lab, VIB Center for Inflammation Research, Brussels, Belgium*
[4]*Nuclear Medicine Department (NUCG), Universitair Ziekenhuis Brussel (UZ Brussel), Brussels, Belgium*

Abstract

Purpose: Macrophage mannose receptor (MMR, CD206) expressing tumor-associated macrophages (TAM) are protumorigenic and was reported to negatively impact therapy responsiveness and is associated with higher chances of tumor relapse following multiple treatment regimens in preclinical tumor models. Since the distribution of immune cells within the tumor is often heterogeneous, sampling "errors" using tissue biopsies will occur. In order to overcome this limitation, we propose positron emission tomography (PET)/X-ray computed tomography (CT) imaging using 68Ga-labeled anti-MMR single-domain antibody fragment (sdAb) to assess the presence of these protumorigenic TAM.

Procedures: Cross-reactive anti-MMR-sdAb was produced according to good manufacturing practice (GMP) and conjugated to *p*-SCN-Bn-NOTA bifunctional chelator for 68Ga-labeling. Biodistribution and PET/CT studies were performed in wild-type and MMR-deficient 3LL-R tumor-bearing mice. Biodistribution data obtained in mice were extrapolated to calculate radiation dose estimates for the human adult using OLINDA software. A 7-day repeated dose toxicity study for NOTA-anti-MMR-sdAb was performed in healthy mice up to a dose of 1.68 mg/kg.

Results: [68Ga]Ga-NOTA-anti-MMR-sdAb was obtained with 76 ± 2 % radiochemical yield, 99 ± 1 % radiochemical purity, and apparent molar activity of 57 ± 11 GBq/μmol. *In vivo* biodistribution analysis showed fast clearance *via* the kidneys and retention in MMR-expressing organs and tumor, with tumor-to-blood and tumor-to-muscle ratios of 6.80 ± 0.62 and 5.47 ± 1.82, respectively. The calculated effective dose was 0.027 mSv/MBq and 0.034 mSv/MBq for male and female, respectively, which means that a proposed dose of 185 MBq in humans would yield a radiation dose of 5.0 and 6.3 mSv to male and female patients, respectively. In the toxicity study, no adverse effects were observed.

Correspondence to: Marleen Keyaerts; *e-mail:* marleen.keyaerts@vub.be

Published online: 22 January 2019

Conclusions: Preclinical validation of [^{68}Ga]Ga-NOTA-anti-MMR-sdAb showed high specific uptake of this tracer in MMR-expressing TAM and organs, with no observed toxicity. [^{68}Ga]Ga-NOTA-anti-MMR-sdAb is ready for a phase I clinical trial.

Key words: Single-domain antibody (sdAb), Macrophage mannose receptor (MMR), Tumor-associated macrophages (TAM), PET

Introduction

Increasing data is becoming available reporting the intense crosstalk between cancer cells and the tumor microenvironment. Tumor-associated macrophages (TAM) in the microenvironment play a key role in tumor growth and progression. Besides local immunosuppression, they influence angiogenesis and cancer cell mobility. Importantly, the TAM population consists of pro- and anti-tumoral populations residing in different tumor regions. In this respect, TAM with a high expression of MMR (MMR^{hi} TAM) were shown to reside in hypoxic tumor areas and were highly angiogenic and strongly immunosuppressive, characteristics that suggest a strong protumoral activity [1–3].

MMR^{hi} TAM were reported to negatively impact therapy responsiveness and allow tumor relapse following irradiation, anti-angiogenic, or vascular disrupting therapies and chemotherapy in preclinical tumor models [4]. A clear association between the presence of MMR^{hi} TAM and the (lack of) responsiveness to treatment has not been demonstrated so far in patients, likely because it is difficult to fully capture the heterogeneity of TAM presence using core needle biopsy and immunohistochemistry (IHC).

To determine MMR^{hi} TAM density, we propose the use of ^{68}Ga-labeled anti-MMR single-domain antibodies fragments (sdAbs) for the non-invasive imaging of MMR^{hi} TAM in all cancer lesions within a patient. sdAbs, such as anti-MMR-sdAbs, are antigen-binding fragments derived from heavy-chain only antibodies of the Camelidae. Compared to conventional antibodies or antibody fragments, sdAbs are small (12–15 kDa) and they have the ability to bind antigens on hidden or unusual epitopes [5]. sdAbs have proven their role in molecular imaging and targeted radionuclide therapy in a preclinical setting [6–9], and a ^{68}Ga-labeled compound for positron emission tomography (PET)/X-ray computed tomography (CT) imaging of HER2 was found safe and it is use straightforward in a phase I clinical trial, with low radiation burden for the patient [10].

Previously, we have reported the generation of cross-reactive anti-mouse/human MMR-sdAbs, selection, and validation of the lead compound for imaging of MMR-expressing macrophages using radiolabeling with ^{99m}Tc and ^{18}F [11]. Here, we report the synthesis and validation of the clinical-grade [^{68}Ga]Ga-NOTA-anti-MMR-sdAb compound for PET/CT imaging, its biodistribution, dosimetry, and toxicity studies in animal models, making [^{68}Ga]Ga-NOTA-anti-MMR-sdAb ready for application in a phase I clinical trial.

Materials and Methods

All commercially obtained chemicals were of analytic grade. *p*-SCN-Bn-NOTA was purchased from Macrocyclics. ^{68}Ga was obtained from a ^{68}Ge/^{68}Ga Galli Eo™ generator (IRE, Belgium). Buffers used for coupling reactions or for radiolabeling were purified from metal contamination using Chelex 100 resin (Aldrich). High purity water (Fluka) was used for radiolabeling.

Production and Purification of GMP-Grade anti-MMR-sdAb

The DNA sequence coding for the cross-reactive human-mouse-anti-MMR-sdAb, described in [11], was cloned in the pAOXZalpha plasmid in frame with the α-factor secretory signal peptide. pAOXZalpha vector is a derivative of the pPICZalpha plasmid (Thermo Fisher), with minor changes in the multiple cloning site. *Pichia pastoris* strain GS115 + His4 was transduced and a clone with stable genomic integration and high sdAb secretion in the medium was selected. The untagged sdAb was purified from the fermenter supernatant by 0.2-µm filtration, mixed-mode chromatography (MMC) capturing and polishing using anion-exchange chromatography (AEX) on NatriFlo a HD-Q Recon column (Natrix). The sdAb was buffer-exchanged to phosphate buffer saline (PBS) by tangential flow filtration and concentrated to 1.9 mg/ml. The GMP-grade sdAb was generated by Q-Biologicals (Ghent).

Chromatographic Analysis

Superdex Peptide 10/300GL (GE), using 0.1 M ammonium acetate pH 7 as eluate and flow 0.5 ml/min, was used for NOTA-anti-MMR-sdAb purification and quality control. Superdex Peptide 3.2/300 column (GE), using 0.02 M PBS/0.28 M NaCl pH 7.4 as mobile phase was used for the quality control of ^{69,71}GaNOTA-anti-MMR-sdAb and [^{68}Ga]Ga-NOTA-anti-MMR-sdAb. The same column was also used when performing stability studies of [^{68}Ga]Ga-NOTA-anti-MMR-sdAb. Instant thin-layer chromatography (iTLC) was performed on silica gel (SG) (Pall Corp. Life Sciences) using 0.1 M sodium citrate pH 5.0 as eluent.

Conjugation of p-SCN-Bn-NOTA to anti-MMR-sdAb

Anti-MMR-sdAb (3 mg, 0.24 µmol) was buffer-exchanged to 0.05 M sodium carbonate buffer, pH 8.7, using PD-10 size exclusion disposable columns (GE). Protein solution (2 ml) was added to a 20-fold molar excess p-SCN-Bn-NOTA (2.6 mg, 47 µmol), pH adjusted to 8.5–8.7 with 0.2 M Na_2CO_3. After 2-h incubation at room temperature (RT), the pH of the reaction mixture is lowered to pH 7.4 by adding HCl 1 N. The NOTA-anti-MMR-sdAb protein solution is loaded on a size exclusion column. The collected fractions containing monomeric NOTA-anti-MMR-sdAb protein are pooled and the solution is passed through a 0.22-µm filter. The protein concentration is determined by UV absorption at 280 nm ($\varepsilon = 40{,}660$ M^{-1} cm^{-1}). Three validation tests were performed in which the product was fully characterized as required for clinical application. Product was stored at -20 °C and stability tests were performed at selected time points (T0M, T3M, T6M at -20 °C and T3d, T7d at 4 °C).

Synthesis of ^{69,71}GaNOTA-anti-MMR-sdAb

To a solution of NOTA-anti-MMR-sdAb (1.2 mg, 91.4 nmol) in 1 ml of 0.1 M ammonium acetate (pH 7), 250 µl of 1 M sodium acetate buffer pH 5 and 35 µl of a 60 mM solution of $Ga(NO_3)_3 \cdot 10H_2O$ (1.83 µmol) were added, and incubated for 2 h at RT. Size exclusion purification using PD-10 column pre-equilibrated with 0.1 M ammonium acetate (pH 7) was used to remove free gallium acetate. ^{69,71}GaNOTA-anti-MMR-sdAb was characterized by ESI-Q-ToF-MS, SDS-PAGE/Western Blot, surface plasmon resonance (SPR), and SEC. The compound was used as the reference for the identification of the radio-SEC chromatogram signals of [^{68}Ga]Ga-NOTA-anti-MMR-sdAb (retention time [t_R] = 8.4 min).

SPR

SPR measurements were performed on a Biacore T200 instrument (GE) as described previously [11].

Preparation of [^{68}Ga]Ga-NOTA-anti-MMR-sdAb

^{68}Ga eluate (500–877 MBq) was added to NOTA-anti-MMR-sdAb (100–130 µg, 7.7–11 nmol) in 1 M sodium acetate buffer pH 5 (1 ml). The homogenized solution is incubated for 10 ± 1 min at RT to form [^{68}Ga]Ga-NOTA-anti-MMR-sdAb. The solution is loaded on a PD-10 column (GE), which is pre-equilibrated with 0.9 % NaCl 5 mg/ml ascorbic acid at pH 6. The column is eluted with 0.9 % NaCl 5 mg/ml ascorbic acid at pH 6 by gravity flow and the eluate is passed through a 0.22-µm filter (Millex GV, Millipore).

Radiochemical purity was evaluated using iTLC and by radio-SEC (SEC: [^{68}Ga]Ga-NOTA-anti-MMR-sdAb $t_R = 10.2$ min; [^{68}Ga]Gacitrate $t_R = 15.9$ min; iTLC-SG: [^{68}Ga]Ga-NOTA-anti-MMR-sdAb $R_f = 0$, [^{68}Ga]Gacitrate $R_f = 1$).

In Vitro Stability of [^{68}Ga]Ga-NOTA-anti-MMR-sdAb

Stability of [^{68}Ga]Ga-NOTA-anti-MMR-sdAb was tested in 0.9 % NaCl 5 mg/ml ascorbic acid at pH 6, with a 1000-fold molar excess diethylenetriaminepentaacetic acid (DTPA) and in human plasma. [^{68}Ga]Ga-NOTA-anti-MMR-sdAb (349 ± 55 MBq, $n = 4$) in 0.9 % NaCl 5 mg/ml ascorbic acid pH 6 at RT was followed by iTLC up to 4 h. [^{68}Ga]Ga-NOTA-anti-MMR-sdAb (22.7 MBq) was added to 500 µl of human plasma incubated at 37 °C up to 1 h and analyzed by SEC. To a solution of [^{68}Ga]Ga-NOTA-anti-MMR-sdAb (22 ± 4 MBq, $n = 2$) was added a 1000-fold molar excess of DTPA and incubated at RT for 4 h and followed by iTLC.

Animal Models

Wild-type (WT) female C57BL/6 mice (Janvier) were used for blood curves (9 weeks old) and dosimetry studies (7 weeks old). To evaluate biodistribution and targeting specificity, female C57BL/6 WT and MMR-deficient (MMR-KO) (Janvier) (7 weeks old) mice were subcutaneously inoculated in the right flank with 3×10^6 of the 3LL-R clone of Lewis lung carcinoma cells suspended in HBSS medium while anesthetized with 2.5 % isoflurane (AB-BOTT). Tumors were allowed to grow for 12 days (tumor weight of 0.662 ± 0.267 g for WT and 0.730 ± 0.268 g for MMR-deficient).

The animals were housed at 22 °C in 50–60 % humidity with a light/dark cycle of 12 h. They were kept under pathogen-free conditions and were given autoclaved food pellets and water *ad libitum*. For animal handling and processing of data, technicians and researchers were not blinded.

All procedures followed the guidelines of the Belgian Council for Laboratory Animal Science and were approved by the Ethical Committee for Animal Experiments of the Vrije Universiteit Brussel (license 13-272-5).

Biodistribution Studies in Tumor-Bearing Mice

3LL-R tumor-bearing mice (C57BL/6 WT ($n = 5$) and MMR-KO ($n = 5$)), anesthetized with 2.5 % isoflurane, were injected intravenously with [^{68}Ga]Ga-NOTA-anti-MMR-sdAb (11.6 ± 0.6 MBq, 5 µg of NOTA-anti-MMR-sdAb) *via* the tail. Mice were euthanized at 3 h after injection, and major organs were collected, weighed, and counted against a standard of known activity in a gamma counter. Tissue/

organ uptake was calculated and expressed as a percentage injected activity (%IA) per gram, corrected for decay.

Blood Curves

WT C57BL/6 mice ($n = 6$) anesthetized with 2.5 % isoflurane were injected intravenously with [^{68}Ga]Ga-NOTA-anti-MMR-sdAb (4.7 ± 0.2 MBq, 5 μg of NOTA-anti-MMR-sdAb) *via* the tail. Blood samples were collected 2, 5, 10, 20, 30, 40, 60, 120, and 180 min after injection, *via* a microcapillary, and analyzed in the gamma counter to obtain a blood time–activity curve. The half-life was calculated by biexponential nonlinear regression fit (GraphPad Prism; GraphPad Software).

Dosimetry Studies

WT C57BL/6 mice ($n = 6$ per time point) anesthetized with 2.5 % isoflurane were injected intravenously with [^{68}Ga]Ga-NOTA-anti-MMR-sdAb (5.1 ± 0.5 MBq, 5 μg of NOTA-anti-MMR-sdAb) *via* the tail. Animals were euthanized at 10, 60, 120, and 180 min post injection and major organs were collected, weighed, and counted against a standard of known activity in a gamma counter. Tissue/organ uptake was calculated and expressed as %IA and %IA/g, corrected for decay. Radiation dose estimates for the adult female and male were calculated from the biodistribution data of mice using OLINDA 1.0 software. Organ doses, effective dose, and effective dose equivalent were calculated using the appropriate weighing factors for the various organs. Full methods are described in supplemental data.

Micro-PET/CT Imaging

Mice were injected with [^{68}Ga]Ga-NOTA-anti-MMR-sdAb (11.62 ± 0.58 MBq, 5 μg NOTA-anti-MMR-sdAb) of the tracer *via* the tail vein, and scanned after 60 and 150 min. Micro-PET/CT imaging was performed on a MILabs VECTor/CT. The CT scan was set to 55 keV and 615 μA, resolution of 80 μm, with a total body scan duration of 108 s. PET images were obtained using the high-energy PET collimator in spiral mode, 94 positions for whole-body imaging, with 9 s per position. Images were reconstructed with 0.6-mm voxels with 4 subsets and 2 iterations, without post reconstruction filter. Image viewing was performed with AMIDE imaging software.

Toxicity Study with NOTA-anti-MMR-sdAb

Full materials and methods of the toxicity study are described in supplemental data. A 7-day intravenous repeated dose toxicity study of the NOTA-anti-MMR-sdAb was performed (Eurofins BioPharma Product testing). The ICH M3 (R2) guideline was applied (*EMA/CPMP/ICH/286/95*).

NOTA-anti-MMR-sdAb or vehicle solution (PBS) was administered at 1.68-mg/kg body weight daily *via* intravenous route to 20 male and 20 female Balb/c mice for 7 days. Toxicity was assessed using observation, blood sampling (hematology and clinical biochemistry), necropsy, and urine analysis. Histopathological examination was performed for 40 selected organs. In addition, 10 recovery animals per group and gender were observed for 14 days following the last administration and were assessed thereafter.

Also, blood cytokine levels were determined in 5 satellite animals per group and per gender at 2 h and 6 h after single administration. Cytokine determination was performed using V-PLEX Plus Proinflammatory Panel 1 (mouse) kit.

Statistical Analysis

Quantitative data are expressed as mean ± SD and compared using the independent t test using Prism 5 (GraphPad Software, Inc.)

Results

Synthesis and Characterization of NOTA-anti-MMR-sdAb and ^{69,71}GaNOTA-anti-MMR-sdAb

The GMP-produced anti-MMR-sdAb was conjugated to *p*-SCN-Bn-NOTA on the ε-amino groups of the lysines forming a thiourea bond. The conjugation reaction resulted in a mixture of molecules with 0 and 1 NOTA chelators, as determined by ESI-Q-ToF-MS analysis. NOTA-anti-MMR-sdAb was characterized and stability studies performed (Suppl. Table 1). The product is stable at 4 °C for at least 7 days, and at −20 °C for at least 6 months. For clinical translation, 3 validation tests of NOTA-anti-MMR-sdAb were performed to confirm the reproducibility of the results (Suppl. Table 2).

^{69,71}GaNOTA-anti-MMR-sdAb was prepared and fully characterized as detailed in Suppl. Table 3. It was subsequently used as a reference compound for [^{68}Ga]Ga-NOTA-anti-MMR-sdAb in SEC and assesses its MMR-binding kinetic parameters.

MMR Protein Binding Characteristics of NOTA-anti-MMR-sdAb and ^{69,71}GaNOTA-anti-MMR-sdAb

SPR experiments were performed on immobilized recombinant human MMR protein to confirm the affinity of chemically modified anti-MMR-sdAb and to determine binding kinetic parameters (Table 1). All compounds bound to the target protein with affinities in the low-nanomolar range, with no pronounced effect from conjugation of the NOTA chelator or complexation with ^{69,71}Ga.

Table 1. Surface plasmon resonance results for the different anti-MMR-sdAb compounds binding to immobilized human recombinant MMR protein

sdAb	k_a (M^{-1} s^{-1})	k_d (s^{-1})	K_D (nM)
anti-MMR-sdAb-His6	3.80×10^5	2.74×10^{-4}	0.72
anti-MMR-sdAb (GMP-produced)	3.33×10^5	2.87×10^{-4}	0.86
NOTA-anti-MMR-sdAb	2.89×10^5	2.90×10^{-4}	1.00
^{69,71}Ga-NOTA-anti-MMR-sdAb	3.88×10^5	5.18×10^{-4}	1.33

k_a, association rate constant; k_d, dissociation rate constant; K_D, equilibrium dissociation constant

Preparation of [^{68}Ga]Ga-NOTA-anti-MMR-sdAb and Stability Studies

NOTA-anti-MMR-sdAb was radiolabeled with ^{68}Ga at RT and pH 5 for 10 min. [^{68}Ga]Ga-NOTA-anti-MMR-sdAb was obtained with a radiochemical yield of 76 ± 2 % ($n = 6$, isolated product after purification, decay corrected), a radiochemical purity of 99 ± 1 % (after purification, iTLC), and an apparent molar activity of 57 ± 11 GBq/μmol (end of purification). The chemical identity of the ^{68}Ga complex ($t_R = 10.2$ min) was confirmed by comparison of the SEC profile with that of the ^{69,71}GaNOTA-anti-MMR-sdAb ($t_R = 8.2$ min). The radiolabeled compound was stable in 0.9 % NaCl 5 mg/ml ascorbic acid at pH 6 and in the presence of 1000-fold molar excess DTPA at RT over 4 h (Table 2). Incubation of the radiolabeled compound in human plasma showed high metabolic stability, as well as high stability with regard to trans-chelation. After 1 h at 37 °C, gel filtration analysis showed that more than 95 % of the activity corresponded to intact compound (Table 2).

In Vivo Biodistribution Studies and Tumor Targeting

The *in vivo* biodistribution of [^{68}Ga]Ga-NOTA-anti-MMR-sdAb was evaluated in WT and MMR-KO mice bearing 3LL-R tumors. Micro-PET/CT imaging showed the highest signal in the kidneys, bladder, liver, and tumor (Fig. 1). Specificity was confirmed since uptake in MMR-expressing organs was negligible in MMR-KO mice. Each labeled sdAb product was used both in WT and KO mice, thereby confirming the absence

of colloids in the injected product, since that would have resulted in non-specific liver uptake in KO mice.

Ex vivo evaluation of the biodistribution (Fig. 2 and Suppl. Table 4, see Electronic Supplementary Material (ESM)) confirmed the specific uptake in MMR-expressing tissues such as the liver, spleen, lymph nodes, bone marrow, and tumor in WT *versus* MMR-KO mice ($p < 0.05$). Tumor-to-blood ratio (T/B) was 6.80 ± 0.62 for WT mice and 1.92 ± 0.69 %IA/g for MMR-KO mice. Similar kidney uptake was observed in both mouse genotypes.

The blood time–activity curve confirmed rapid clearance of [^{68}Ga]Ga-NOTA-anti-MMR-sdAb from the blood, yielding a biphasic blood curve (Suppl. Fig. 1 in ESM) with half-lives of the initial phase of 1.2 min (distribution phase) and that of the slow phase of 21.7 min (elimination phase). The biological half-life was calculated as 2.49 h using the whole-body time–activity curve (excluding bladder activity) and using a mono-exponential trend line (Suppl. Fig. 2 in ESM).

Dosimetry Analysis

An estimation of organ-absorbed doses was performed by extrapolation of the biodistribution data of [^{68}Ga]Ga-NOTA-anti-MMR-sdAb at different time points in mice (Suppl. Table 5 in ESM) to the human male and female adult phantom using OLINDA software (Table 3). The organ-absorbed doses were calculated using a voiding bladder model with 100 % renal clearance, a voiding bladder interval of 1 h and the biological half-life of 2.49 h. Table 3 summarizes the organ-absorbed doses. The effective dose was estimated at 0.0270 mSv/MBq for male and 0.0342 mSv/MBq for female, which means that a proposed patient dose of 185 MBq would yield an estimated radiation dose of 5.0 mSv and 6.3 mSv to male and female patients, respectively.

Toxicity Study of NOTA-anti-MMR-sdAb

Overall, no treatment-related toxicologically relevant changes were observed in clinical signs, growth, hematology, clinical chemistry, organ weights, gross macroscopy,

Table 2. *In vitro* stability of [^{68}Ga]Ga-NOTA-anti-MMR-sdAb

Incubation condition		Radioactivity in [^{68}Ga]Ga-NOTA-anti-MMR-sdAb (%)*	Method of analysis
Medium	Time (h) and temperature		
0.9 % NaCl 5 mg/ml ascorbic acid pH 6	1 h, RT	97 ± 1	iTLC
	2 h, RT	97 ± 1	iTLC
	3 h, RT	96 ± 2	iTLC
	4 h, RT	98	iTLC
Human plasma	1 h, 37 °C	> 95	SEC
1000-fold molar excess DTPA	1 h, RT	97 ± 1	iTLC
	4 h, RT	96	iTLC

*% of the total applied radioactivity associated with the [^{68}Ga]Ga-NOTA-anti-MMR-sdAb peak or spot after incubation in the applied condition
RT, room temperature; *iTLC*, instant thin-layer chromatography; *SEC*, size exclusion chromatography; *DTPA*, diethylenetriaminepentaacetic acid
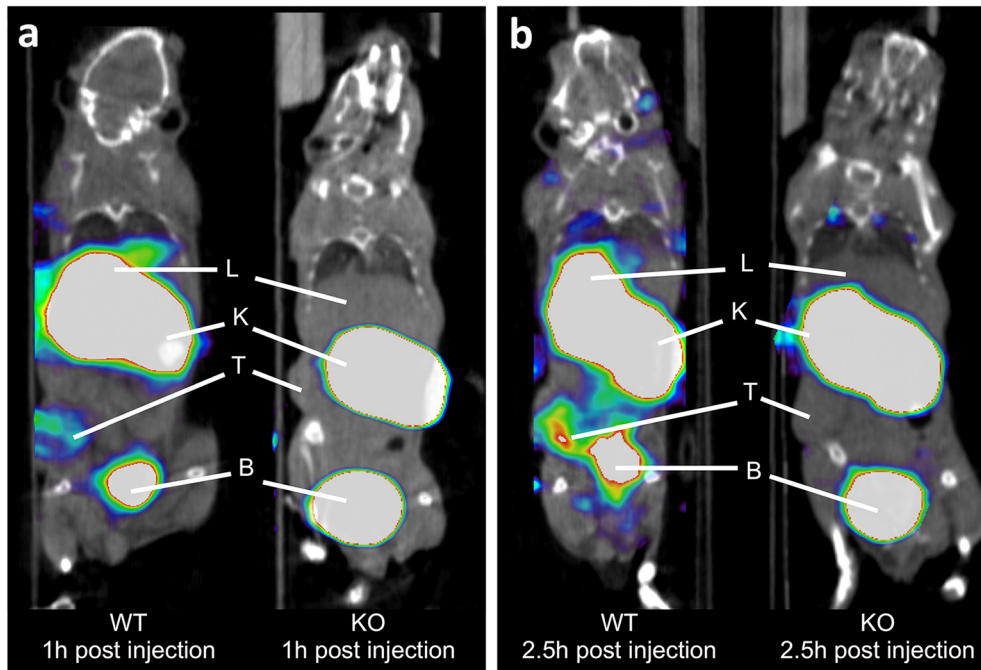
Fig. 1. Coronal PET/CT images of wild-type (WT) *versus* MMR-deficient (KO) 3LL-R tumor-bearing mice scanned at **a** 1h and **b** 2.5h post injection of [^{68}Ga]Ga-NOTA-anti-MMR-sdAb. PET signals are encoded in color scale, CT image in gray scale. T, tumor; K, kidney; L, liver; B, bladder.

and microscopic observations. Based on the absence of treatment-related toxicologically relevant changes in the endpoints examined, the no observed effect level (NOEL) could be established to be > 1.68 mg/kg body weight. Moreover, at the dose tested, NOTA-anti-MMR-sdAb was well tolerated at the injected site and not associated with any acute immunological reaction.

Discussion

In oncology research, increasing attention is going to the tumor microenvironment, with a high interest in the local immune interactions, to better understand primary and acquired resistance to different types of immunotherapy. It is hypothesized that the *in vivo* imaging of key molecular markers such as programmed death-ligand 1 (PD-L1) and
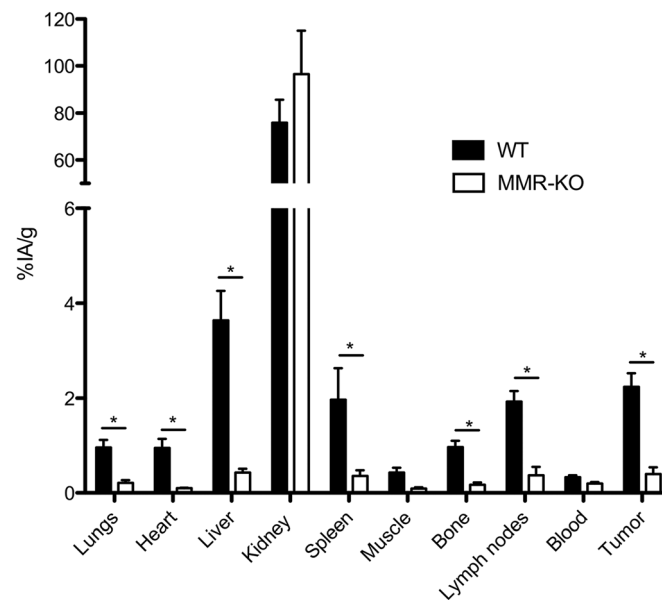
Fig. 2. Biodistribution of [^{68}Ga]Ga-NOTA-anti-MMR-sdAb, in wild-type (WT) and MMR-deficient (MMR-KO) mice bearing 3LL-R tumors at 3-h post injection. Data are expressed as mean %IA/g $\pm$ SD ($n = 5$); dose of protein (NOTA-anti-MMR-sdAb) injected was 5 μg. $*p < 0.05$.

Table 3. Radiation dose estimates to different organs for the adult male and female humans based on OLINDA calculations

Target organ	Organ dose adult male (mGy/MBq)	Organ dose adult female (mGy/MBq)
Adrenals	0.0107	0.0135
Brain	0.0005	0.0006
Breasts	0.0031	0.0039
Gallbladder wall	0.0109	0.0127
Lower large intestine wall	0.0194	0.0219
Small intestine	0.0158	0.0188
Stomach wall	0.0120	0.0141
Upper large intestine wall	0.0149	0.0175
Heart wall	0.0074	0.0096
Kidneys	0.447	0.486
Liver	0.0395	0.0526
Lungs	0.0040	0.0052
Muscle	0.0044	0.0055
Ovaries		0.0082
Pancreas	0.0084	0.0102
Red marrow	0.0045	0.0054
Osteogenic cells	0.0051	0.0069
Skin	0.0032	0.0040
Spleen	0.0250	0.0305
Testes	0.0042	
Thymus	0.0194	0.0205
Thyroid	0.0024	0.0028
Urinary bladder wall	0.170	0.229
Uterus		0.0101
Total body	0.0074	0.0094
Effective dose equivalent (mSv/MBq)	0.0437	0.0534
Effective dose (mSv/MBq)	0.0270	0.0342

tumor-infiltrating lymphocytes can help to understand such resistance mechanisms [12]. Also TAM are believed to play a role in primary resistance to immunotherapy. Macrophages found in the tumor microenvironment display a broad spectrum of molecular markers, and some of these markers are associated with a protumoral and immune-suppressive behavior. As such, macrophage mannose receptor (MMR) has been identified as a distinct marker, present on M2-polarized TAM that promote tumor growth and metastasis and inhibit local immune activation [1–3]. The presence of such MMR-expressing TAM could therefore be indicative for the success rate of immune-activating therapies. To further investigate this role in cancer patients, we have developed a PET/CT imaging method using an MMR-targeting sdAb and ^{68}Ga-labeling enabling PET/CT quantification.

The MMR-specific sdAb that recognizes both the mouse and the human MMR target was GMP-produced without any c-terminal tag. The bifunctional chelator p-SCN-Bn-NOTA was conjugated to the GMP-grade compound and radiolabeled with [68]Ga. The compound proved to be stable both in the final buffer and in human plasma, and the compound was resistant to trans-chelation, confirming high stability of the [^{68}Ga]Ga-NOTA complex. The affinity of the different compounds was around 1 nM and not affected either by conjugation of NOTA or complexation with [69,71]Ga. These *in vitro* characterization tests confirm its suitability for further translation to patient use.

In mice, [^{68}Ga]Ga-NOTA-anti-MMR-sdAb accumulate specifically in MMR-expressing organs such as the liver and spleen, as well as in the 3LL-R tumors that are known to be infiltrated with high amounts of MMR[hi] TAM [1]. Specificity was confirmed by the absence of signal in MMR-deficient mice (MMR-KO), both in healthy organs and in 3LL-R tumors. The tracer was rapidly cleared from the blood *via* the kidneys and urine, as observed by both PET/CT imaging and *ex vivo* biodistribution analysis. The confirmation of specific targeting and rapid clearance of unbound compound provides the necessary evidence of its potential added value for subsequent use in patients.

When comparing uptake values of the [^{68}Ga]Ga-NOTA-anti-MMR-sdAb with the previously reported [^{99m}Tc]Tc(CO)$_3$-anti-MMR-sdAb and [^{18}F]FB-anti-MMR-sdAbs, the tumor uptake for all three compounds is very similar in WT 3LL-R tumor-bearing mice [11]. Uptake in extra-tumoral MMR-expressing organs, such as the liver, spleen, lymph nodes, and bone, is slightly higher for the [68]Ga- compound when compared to the ^{18}F version, but substantially lower than what was observed for the ^{99m}Tc compound. These differences may be due to different radiochemistry methods or differences in apparent molar activity (70.1, 31.5, 10.1 GBq/μmol for ^{99m}Tc, ^{68}Ga, ^{18}F, respectively (injection time)) [11]. Kidney uptake was also different for the three variants, with the lowest value obtained for the [^{18}F]FB-anti-MMR-sdAb (7.98 ± 0.86 %IA/g at 3 h p.i.), which is about 20-fold lower than that seen with [^{99m}Tc]Tc(CO)$_3$-anti-MMR-sdAb and 10-fold lower than with the here presented [^{68}Ga]Ga-NOTA-anti-MMR-sdAb [11]. Similar lower kidney retention for ^{18}F-labeled sdAb has also been reported for anti-HER2, although

only for the [^{18}F]FSB, and not using [^{18}F]RL-I prosthetic group, confirming that the radiochemistry is a defining factor [13–15]. Depending on the chemical structure created, different catabolites will be produced in the kidney cells, with some ^{18}F-catabolites clearing faster from kidneys. Although the [^{18}F]FB-anti-MMR-sdAb compound holds promise for clinical translation and might even perform better given its lower kidney retention, our research group has chosen to initiate clinical trials with the [^{68}Ga]Ga-NOTA-anti-MMR-sdAb because of the ease of production and radiolabeling that could be implemented in many radiopharmacies worldwide, even in the absence of cyclotrons or synthesis modules.

For subsequent human use of [^{68}Ga]Ga-anti-MMR-sdAb, the average radiation dose for a human adult was estimated based on extrapolation of normal distribution and retention in mice. The average effective dose was 0.034 and 0.027 mSv/MBq for female and male respectively, resulting in a total body radiation dose per injection of 185 MBq of ^{68}Ga compound of 6.3 and 5.0 mSv for female and male, respectively. The organs that would receive the highest dose are the kidneys (up to 90 mGy) and the urinary bladder wall (up to 42 mGy), staying well below the kidney threshold of 7–8 Gy for potential deterministic effects [16]. The total body irradiation dose is in the same range as a standard 2-deoxy-2-[^{18}F]fluoro-D-glucose PET scan (7 mSv for 370 MBq of administered activity), and could be used in daily clinical practice for diagnosis and follow-up of patients. In the toxicity study, NOTA-anti-MMR-sdAb showed no adverse effects after the 7-day repeated injected up to a dose of 1.68 mg/kg. This dose is a 1000-fold excess of what a 60-kg patient would receive when injected with 0.1 mg of the compound. Based on all preclinical data reported here, [^{68}Ga]Ga-NOTA-anti-MMR-sdAb can be regarded as safe for clinical translation. A phase I trial to assess safety, biodistribution and dosimetry in cancer patients will be initiated in the near future.

Other research groups have also investigated macrophage imaging using mannose receptor targeting. Many have focused on mannosylation of the targeting moiety, thereby utilizing the natural ligand of MMR [17–19]. However, mannose does not only bind MMR, but also multiple other mannose-binding proteins, such as mannose-binding lectins. Such lectins are serum proteins that will bind to mannose and other types of sugars that occur on the cell surface of bacteria and yeasts, thereby facilitating opsonization by phagocytes. It can be foreseen that using mannosylated compounds for imaging will therefore not only identify MMR-expressing macrophages, but will also target other phagocytes that will engulf lectin-bound compounds.

Fluorescence imaging using more specific MMR-targeting agents has been reported using a full monoclonal anti-MMR antibody and using an MMR-binding peptide [20–22]. Recently, a ^{125}I-labeled monoclonal antibody was used for SPECT imaging [22]. These studies confirm the promise of specifically targeting MMR for the imaging of protumorigenic macrophages, but the use of sdAb offers multiple advantages compared to approaches using mAbs given their faster blood clearance and good tissue penetration characteristics.

Conclusions

In conclusion, the [^{68}Ga]3Ga-NOTA-anti-MMR-sdAb is a very interesting PET tracer with a high potential to specifically image the protumorigenic macrophages in the tumor microenvironment in patients. Its safety and efficacy have been confirmed in mouse studies and the extrapolated radiation doses are within acceptable ranges for repeated imaging. The envisioned trials in cancer patients will help to define the role of MMR^{hi} TAM in cancer progression and its susceptibility to immuno-oncological treatments.

Conflict of Interest

Publisher's note Springer Nature remains neutral with regard to jurisdictional claims in published maps and institutional affiliations.

References

1. Laoui D, Van Overmeire E, Di Conza G et al (2014) Tumor hypoxia does not drive differentiation of tumor-associated macrophages but rather fine-tunes the M2-like macrophage population. Cancer Res 74:24–30
2. Movahedi K, Laoui D, Gysemans C, Baeten M, Stange G, van den Bossche J, Mack M, Pipeleers D, in't Veld P, de Baetselier P, van Ginderachter JA (2010) Different tumor microenvironments contain functionally distinct subsets of macrophages derived from Ly6C(high) monocytes. Cancer Res 70:5728–5739

3. Movahedi K, Schoonooghe S, Laoui D, Houbracken I, Waelput W, Breckpot K, Bouwens L, Lahoutte T, de Baetselier P, Raes G, Devoogdt N, van Ginderachter JA (2012) Nanobody-based targeting of the macrophage mannose receptor for effective in vivo imaging of tumor-associated macrophages. Cancer Res 72:4165–4177

4. De Palma M, Lewis CE (2013) Macrophage regulation of tumor responses to anticancer therapies. Cancer Cell 23:277–286

5. Krasniqi A, D'Huyvetter M, Devoogdt N et al (2018) Same-day imaging using small proteins: clinical experience and translational prospects in oncology. J Nucl Med 59:885–891

6. D'Huyvetter M, De Vos J, Xavier C et al (2017) ^{131}I-labeled anti-HER2 camelid sdAb as a theranostic tool in cancer treatment. Clin Cancer Res 23(21):6616–6628

7. D'Huyvetter M, Vincke C, Xavier C, Aerts A, Impens N, Baatout S, de Raeve H, Muyldermans S, Caveliers V, Devoogdt N, Lahoutte T (2014) Targeted radionuclide therapy with A 177Lu-labeled anti-HER2 nanobody. Theranostics 4:708–720

8. Xavier C, Vaneycken I, D'Huyvetter M et al (2013) Synthesis, preclinical validation, dosimetry, and toxicity of ^{68}Ga-NOTA-anti-HER2 Nanobodies for iPET imaging of HER2 receptor expression in cancer. J Nucl Med 54:776–784

9. Broos K, Keyaerts M, Lecocq Q, Renmans D, Nguyen T, Escors D, Liston A, Raes G, Breckpot K, Devoogdt N (2017) Non-invasive assessment of murine PD-L1 levels in syngeneic tumor models by nuclear imaging with nanobody tracers. Oncotarget 8:41932–41946

10. Keyaerts M, Xavier C, Heemskerk J, Devoogdt N, Everaert H, Ackaert C, Vanhoeij M, Duhoux FP, Gevaert T, Simon P, Schallier D, Fontaine C, Vaneycken I, Vanhove C, de Greve J, Lamote J, Caveliers V, Lahoutte T (2016) Phase I study of ^{68}Ga-HER2-Nanobody for PET/CT assessment of HER2 expression in breast carcinoma. J Nucl Med 57:27–33

11. Blykers A, Schoonooghe S, Xavier C, D'hoe K, Laoui D, D'Huyvetter M, Vaneycken I, Cleeren F, Bormans G, Heemskerk J, Raes G, de Baetselier P, Lahoutte T, Devoogdt N, van Ginderachter JA, Caveliers V (2015) PET imaging of macrophage mannose receptor-expressing macrophages in tumor stroma using ^{18}F-radiolabeled camelid single-domain antibody fragments. J Nucl Med 56:1265–1271

12. Kim TK, Herbst RS, Chen L (2018) Defining and understanding adaptive resistance in cancer immunotherapy. Trends Immunol 39:642–631

13. Vaneycken I, Devoogdt N, Van Gassen N et al (2011) Preclinical screening of anti-HER2 nanobodies for molecular imaging of breast cancer. FASEB J 25:2433–2446

14. Xavier C, Blykers A, Vaneycken I, D'Huyvetter M, Heemskerk J, Lahoutte T, Devoogdt N, Caveliers V (2016) ^{18}F-nanobody for PET imaging of HER2 overexpressing tumors. Nucl Med Biol 43:247–252

15. Zhou Z, Vaidyanathan G, McDougald D, Kang CM, Balyasnikova I, Devoogdt N, Ta AN, McNaughton BR, Zalutsky MR (2017) Fluorine-18 labeling of the HER2-targeting single-domain antibody 2Rs15d using a residualizing label and preclinical evaluation. Mol Imaging Biol 19:867–877

16. Stewart FA, Akleyev AV, Hauer-Jensen M et al (2012) ICRP publication 118: ICRP statement on tissue reactions and early and late effects of radiation in normal tissues and organs–threshold doses for tissue reactions in a radiation protection context. Ann ICRP 41:1–322

17. Jiang C, Cai H, Peng X et al (2017) Targeted imaging of tumor-associated macrophages by cyanine 7-labeled mannose in xenograft tumors. Mol Imaging 16. https://doi.org/10.1177/1536012116689499

18. Lee SP, Im HJ, Kang S, Chung SJ, Cho YS, Kang H, Park HS, Hwang DW, Park JB, Paeng JC, Cheon GJ, Lee YS, Jeong JM, Kim YJ (2017) Noninvasive imaging of myocardial inflammation in myocarditis using ^{68}Ga-tagged mannosylated human serum albumin positron emission tomography. Theranostics 7:413–424

19. Varasteh Z, Hyafil F, Anizan N, Diallo D, Aid-Launais R, Mohanta S, Li Y, Braeuer M, Steiger K, Vigne J, Qin Z, Nekolla SG, Fabre JE, Döring Y, le Guludec D, Habenicht A, Vera DR, Schwaiger M (2017) Targeting mannose receptor expression on macrophages in athero-sclerotic plaques of apolipoprotein E-knockout mice using ^{111}In-tilmanocept. EJNMMI Res 7:40

20. Scodeller P, Simon-Gracia L, Kopanchuk S et al (2017) Precision targeting of tumor macrophages with a CD206 binding peptide. Sci Rep 7:14655

21. Sun X, Gao D, Gao L, Zhang C, Yu X, Jia B, Wang F, Liu Z (2015) Molecular imaging of tumor-infiltrating macrophages in a preclinical mouse model of breast cancer. Theranostics 5:597–608

22. Zhang C, Yu X, Gao L, Zhao Y, Lai J, Lu D, Bao R, Jia B, Zhong L, Wang F, Liu Z (2017) Noninvasive imaging of CD206-positive M2 macrophages as an early biomarker for post-chemotherapy tumor relapse and lymph node metastasis. Theranostics 7:4276–4288